SHORT TERM DEFLECTION OF ORDINARY, PARTIALLY PRESTRESSED AND GFRP BARS REINFORCED CONCRETE BEAMS

Assis Prof. Dr. Nazar K. Ali Oukaili, Iqbal Fadhil Peera Al-Hawwassi,
Civil Engineering Department,
College of Engineering, University of Baghdad

ABSTRACT

The behavior of structural concrete beams is studied under short-term loading. A computer program developed originally by Oukaili to evaluate curvature is modified to evaluate the deflection for flexural structural concrete members. The program deals with actual stress-strain relationships of concrete and steel. The analysis is based on requirements of equilibrium and compatibility of strain in concrete and reinforcement. The proposed model is used in conjunction with the step by step analysis for small loading increments that allows the determination of the history of strain and stress in concrete with prestressing steel or non-prestressing reinforcement only or prestressing and non-prestressing reinforcement together. The evaluation of curvatures for the structural member involves iterations for computing the strains vectors at each analysis step. Newmark's numerical integration is used to evaluate the deflection of the member depending on the curvature values. The stress-strain model that was proposed by (Korpenko et al. 1986) is used and compared with experimental data and other analytical models for each of concrete and steel. The comparison showed good agreement between the model used and the experimental data. This relationship is used in SECTION program and presented in this study. The analytical results for load-deflection diagram are compared with available experimental data. The comparison has shown good agreement.

الهطول قصير الأمد للعتبات الخرسانية المسلحة العادية والمسبقة الجهد جزئياً و المسلحة بقضبان ألياف الزجاج

الخلاصة

في هذا البحث درست سلوكية العتبات الخرسانية تحت تأثير الأحمال قصيرة الأمد. حيث تم تطوير برنامج أقترحه سابقاًالعقيلي لغرض حساب قيم الهطول لأعضاء الخرسانة الإنشائية المعرضة للإنحناء. إنّ البرنامج المعتمد يأخذ في الإعتبار مخططات الإجهاد-الإنفعال الفعلية في الخرسانة و الحديد.إنّ طبيعة التحليل تعتمد على شروط الإتزان و التوافق في الإنفعالات في الخرسانة وفي التسليح. يقترن النموذج المدروس مع التحليل الخطوي و ذلك بإستخدام التحميل على مراحل صغيرة مما يتيح إمكانية دراسة تزايد الإنفعال و الإجهاد في المقطع الخرساني وحديد التسليح الموجود، سواء كان الحديد المستخدم مجهد سابقاً أو حديد غير مجهد سابقاً فقط ، أو حديد قسم مجهد سابقاً وقسم غير مجهد سابقاً سوية. إنّ إسلوب تحديد التقوس(curvature) للعنصر الإنشائي يتضمن عمليات تكرارية هدفها إيجاد قيمة الإنفعالات العمودية في كل مرحلة تحميل. تم إستخدام طريقة Newmark لغرض التكامل لقيم التقوس للمقاطع المدروسة على إمتداد العتبة لغرض إيجاد قيم الهطول لكل نقطة على طول العتبة. تمت مقارنة النتائج الخاصة بقيم الإجهاد-الإنفعال لكلٍ من الخرسانة و الحديد مع بيانات مختبرية ونماذج نظرية لباحثين آخرين، وقد وجد إنّ الأنموذج المستخدم لتمثيل الإجهاد-الإنفعال و المقترح من قبل الباحث Korpenko واخرين يعطي توافقاً جيداً لكلا المادتين.

أستُخدِم هذا الأنموذج في البرنامج المقدم (SECTION program) .إنّ النتائج النظرية الخاصة بقيم الحمل-الهطول للعتبات تمت مقارنتها أيضاً مع نتائج مختبرية متوفرة . لقد وجد إن هناك توافقاً جيداً بين النتائج العملية و النظرية لقيم الهطول.

KEYWORDS: Beam, Reinforced concrete, Prestressed concrete, GFRP, Deflection, Curvature, Stress-Strain, Korpenko, Newmark

INTRODUCTION

Deflection is defined according to **(ACI 116, 2000)** as a movement of a point on a structure or structural element, usually measured as a linear displacement or as succession of displacements transverse to a reference line or axis. There are many empirical and analytical methods for computing deflection of structural concrete members. In this paper an analytical method is modified to compute the deflection of a structural concrete member based on the materials stress-strain relationships, the curvature of the cross-section is determined according to these stress-strain relationships, and then integration is made for the cross-section curvatures along the beam to determine the deflection. It must be mentioned that this analytical method takes into consideration the effect of tension stiffening after cracking of concrete. This analytical model is compared to the available experimental data and hand calculations.

STRESS-STRAIN MODEL

Stress-strain model for concrete

In 1986, Korpenko published a descriptive relationship for $\sigma - \varepsilon$ diagrams, which became very famous because of its overcoming of major deficient problems as shown in Fig. (1).

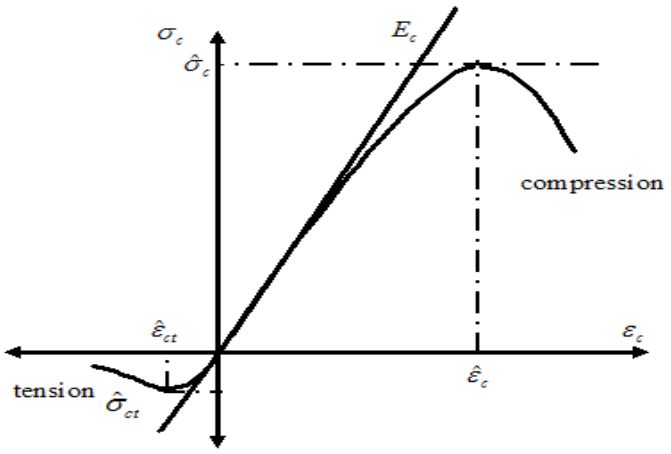

Figure (1) Stress-strain diagram for concrete in compression and tension (Korpenko et al., 1986)

It is taken that σ_c be the stress, ε_c the relative strain, E_c the initial modulus of elasticity, c referring to concrete in compression, and ct to concrete in tension.

Instead of using σ_c and ε_c , it is easier to use the level of each one according to the relationship indicated below:

$$\tilde{\sigma}_c = \left|\frac{\sigma_c}{\hat{\sigma}_c}\right| \quad ; \tilde{\varepsilon}_c = \left|\frac{\varepsilon_c}{\hat{\varepsilon}_c}\right| \tag{1}$$

where: $\tilde{\sigma}_c$ =concrete stress level, $\tilde{\varepsilon}_c$ =concrete strain level, $\hat{\sigma}_c$ =ultimate compressive strength of concrete, $\hat{\varepsilon}_c$ =the concrete strain corresponding to $\hat{\sigma}_c$.

At the beginning of $\sigma - \varepsilon$ diagram, a linear portion can be recognized which extends up to the stress $\sigma_{c,el}$ and the strain $\varepsilon_{c,el}$ or even until their levels $\tilde{\sigma}_{c,el}$ which is equal to $\frac{\sigma_{c,el}}{\hat{\sigma}_c}$ and $\tilde{\varepsilon}_{c,el}$ which is equal to $\frac{\varepsilon_{c,el}}{\hat{\varepsilon}_c}$ .The stress in concrete can be expressed as:

$$\sigma_c = \varepsilon_c E_c \nu_c \tag{2}$$

ν_c is concrete elastic modulus factor that expresses the ratio of elastic strains to the total strains.

$$\nu_c = 1 \qquad \text{if} \quad |\sigma_c| \le |\sigma_{c,el}| \tag{3}$$

$$\nu_c^{\,2}\left[1+\frac{e_{2c}(\nu_o-\hat{\nu}_c)^2\cdot\tilde{\varepsilon}_c^{\,2}}{\hat{\nu}_c(1-\tilde{\sigma}_{c,el})^2}\right]-\nu_c\left[2\hat{\nu}_c-\frac{\tilde{\varepsilon}_c(\nu_o-\hat{\nu}_c)^2}{\hat{\nu}_c(1-\tilde{\sigma}_{c,el})}\left(e_{1c}-\frac{2e_{2c}\tilde{\sigma}_{c,el}}{1-\tilde{\sigma}_{c,el}}\right)\right] \qquad \text{if} \quad |\sigma_c| > |\sigma_{c,el}| \tag{4}$$

$$+\hat{\nu}_c^{\,2}-(\nu_o-\hat{\nu}_c)^2\left[1+\frac{e_{1c}\tilde{\sigma}_{c,el}}{1-\tilde{\sigma}_{c,el}}-\frac{e_{2c}\tilde{\sigma}_{c,el}^{\,2}}{(1-\tilde{\sigma}_{c,el})^2}\right]=0$$

By solving the second degree formula, two roots are obtained from the formula; the larger root is taken for ν_c .

$$\tilde{\sigma}_c = \left|\frac{\sigma_c}{\hat{\sigma}_c}\right|; \tilde{\varepsilon}_c = \left|\frac{\varepsilon_c}{\hat{\varepsilon}_c}\right|, \quad \eta_c = \frac{\sigma_c - \sigma_{c,el}}{\hat{\sigma}_c - \sigma_{c,el}} = \frac{\tilde{\sigma}_c - \tilde{\sigma}_{c,el}}{1-\tilde{\sigma}_{c,el}} \le 1 \quad , \quad \hat{\nu}_c = \frac{\hat{\sigma}_c}{\left|\hat{\varepsilon}_c\right| E_c}$$

where: $\hat{\nu}_c = \nu_c$ value when $\sigma_c = \hat{\sigma}_c$ (at the top of stress-strain diagram).

ν_o factor which depends on stress level in the material (concrete in this case).

ν_o =1 if $\tilde{\varepsilon}_c \le 1$

ν_o =$2.05\hat{\nu}_c$ if $\tilde{\varepsilon}_c > 1$

e_{1c} , e_{2c} are factors which express the type of the concrete.

e_{1c} =1.72 -1.82$\hat{\nu}_c$ if $\tilde{\varepsilon}_c \le 1$

e_{1c} =1.95$\hat{\nu}_c$ -0.138 if $\tilde{\varepsilon}_c > 1$

$e_{2c} = 1 - e_{1c}$

From the conditions of Eq. (4) that is $e_{1c} < 2$

$$\left|\hat{\varepsilon}_c\right| \approx 0.002 \quad ; \quad \tilde{\sigma}_{c,el} = 0 \quad ; \tilde{\varepsilon}_{c,el} = 0 \quad , \quad \tilde{\sigma}_c = \tilde{\varepsilon}_c \nu_c / \tilde{\nu}_c$$

Stress-strain model for steel

σ_s is written to be the stress, ε_s the relative strain (elongation), E_s the initial modulus of elasticity for steel, and s to refer to the steel.

When mild steel enters the stiffness region, it is advised to use the bilinear diagram that is of two branches, one ends at the point of yield region (with coordinates $\varepsilon_s = \hat{\varepsilon}_s$, $\sigma_s = \hat{\sigma}_s$), and the other begins from the end of the first branch to reach the point of coordinates $\sigma_s = \sigma_s^*$, $\varepsilon_s = \varepsilon_s^*$,which corresponds to the ultimate strength or failure limit as shown in Fig. (2).
Mild steel can be represented by the following equations:

$$\sigma_s = \varepsilon_s E_s \nu_s \tag{5}$$

$$\nu_s = 1 \qquad \text{if} \qquad \left|\sigma_s\right| \le \left|\sigma_{s,el}\right|$$

(6)

$$\nu_s^2\left[1+\frac{e_{2s}(\nu_o-\hat{\nu}_s)^2\cdot\tilde{\varepsilon}_s^{\,2}}{\hat{\nu}_s(1-\tilde{\sigma}_{s,el})^2}\right]-\nu_s\left[2\hat{\nu}_s-\frac{\tilde{\varepsilon}_s(\nu_o-\hat{\nu}_s)^2}{\hat{\nu}_s(1-\tilde{\sigma}_{s,el})}\left(e_{1s}-\frac{2e_{2s}\tilde{\sigma}_{s,el}}{1-\tilde{\sigma}_{s,el}}\right)\right]$$
$$+\hat{\nu}_s^{\,2}-(\nu_o-\hat{\nu}_s)^2\left[1+\frac{e_{1s}\tilde{\sigma}_{s,el}}{1-\tilde{\sigma}_{s,el}}-\frac{e_{2s}\tilde{\sigma}_{s,el}^{\,2}}{(1-\tilde{\sigma}_{s,el})^2}\right]=0 \qquad \text{if} \qquad \left|\sigma_s\right| \succ \left|\sigma_{s,el}\right| \tag{7}$$

By solving the second degree formula, two roots are obtained from the formula; the larger root is taken for ν_c . Thus:

$$e_{1s}=\frac{(\nu_o-\hat{\nu}_s)^2(\eta_{s(c)}^{\,2}-1)+(\nu_{s(c)}-\hat{\nu}_s)^2}{(\eta_{s(c)}^{\,2}-\eta_{s(c)})(1-\hat{\nu}_s)^2}\le 2$$

$$\sigma_{s(c)} \approx 1.2\sigma_y \,, \varepsilon_{s(c)} = 0.05 + \frac{\sigma_{s(c)}}{E_s} \,, \ \eta_{s(c)} = \frac{\sigma_{s(c)} - \hat{\sigma}_s}{\sigma^*{}_s - \hat{\sigma}_s} \,, \ \nu_{s(c)} = \frac{\sigma_{s(c)}}{E_s \varepsilon_{s(c)}}$$

$$\eta_s = \frac{\sigma_s - \sigma_{s,el}}{\hat{\sigma}_s - \sigma_{s,el}} = \frac{\tilde{\sigma}_s - \tilde{\sigma}_{s,el}}{1 - \tilde{\sigma}_{s,el}} \le 1 \,, \ \tilde{\sigma}_s = \frac{\sigma_s}{\sigma^*{}_s} \,, \tilde{\varepsilon}_s = \frac{\varepsilon_s}{\varepsilon^*{}_s} \ , \ \nu_o = \frac{\hat{\sigma}_s}{E_s \hat{\varepsilon}_s} \,, \ \hat{\nu}_s = \frac{\sigma^*{}_s}{E_s \varepsilon^*{}_s} \,,$$

$\hat{\varepsilon}_s = \frac{\hat{\sigma}_s}{E_s} + \lambda_y$, $\lambda_y =$ yield plateau length = (0.008-0.015) according to steel type.

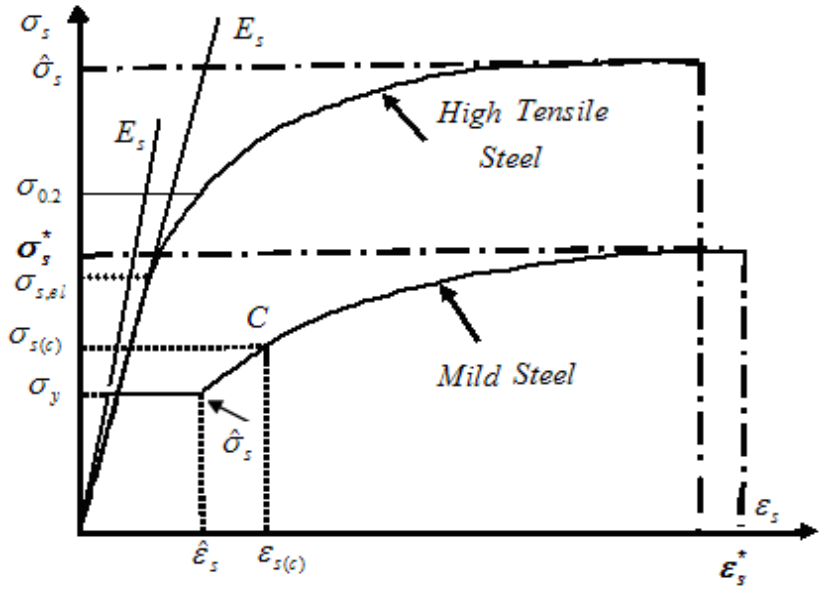

Figure (2) Stress-strain diagram of mild and high strength steel (Korpenko et al., 1986)

For high strength steel the same equations (5, 6, 7) are used but

$$e_{1s}=\frac{(\nu_o-\hat{\nu}_s)^2(\eta_{0.2}^2-1)+(\nu_{0.2}-\hat{\nu}_s)^2}{(\eta_{0.2}^2-\eta_{0.2})(1-\hat{\nu}_s)^2}\le 2$$

$$\varepsilon_{0.2}=\frac{\sigma_{0.2}}{E_s}+0.002\ ,\ \nu_{0.2}=\frac{\sigma_{0.2}}{E_s\varepsilon_{0.2}}\ ,\ \eta_{0.2}=\tilde{\sigma}_{0.2}\frac{1-\beta_{el}}{1-\beta_{el}\cdot\tilde{\sigma}_{0.2}}\ ,$$

$$\hat{\nu}_s=\frac{\hat{\sigma}_s}{E_s\hat{\varepsilon}_s}\ ,\ \sigma_{s,el}=\beta_{el}\cdot\sigma_{0.2}\ ,\ \nu_o=1$$

$$\eta_s=\frac{\sigma_s-\sigma_{s,el}}{\hat{\sigma}_s-\sigma_{s,el}}=\frac{\tilde{\sigma}_s-\tilde{\sigma}_{s,el}}{1-\tilde{\sigma}_{s,el}}\le 1,\tilde{\sigma}_s=\frac{\sigma_s}{\hat{\sigma}_s},\tilde{\varepsilon}_s=\frac{\varepsilon_s}{\hat{\varepsilon}_s}\ ,$$

Stress-strain model for FRP

The stress-strain diagram for FRP is assumed linearly elastic until failure stage as shown in (Fig. 3).

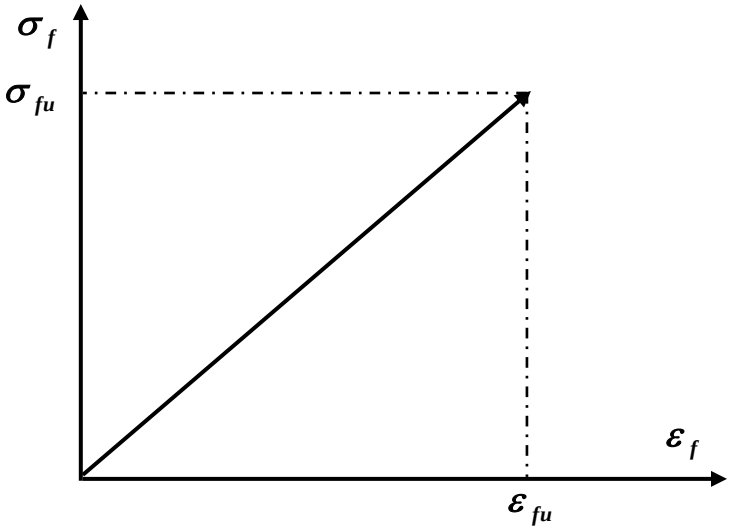

Figure (3) Stress-strain diagram for FRP

Comparison of the stress-strain relationships of the materials

The proposed stress-strain model is compared to other models by using available experimental data for concrete (LSC, NSC, HSC) and for steel with its types mild; high strength; and high strength for prestressing as shown in Figures from (4) to (12).

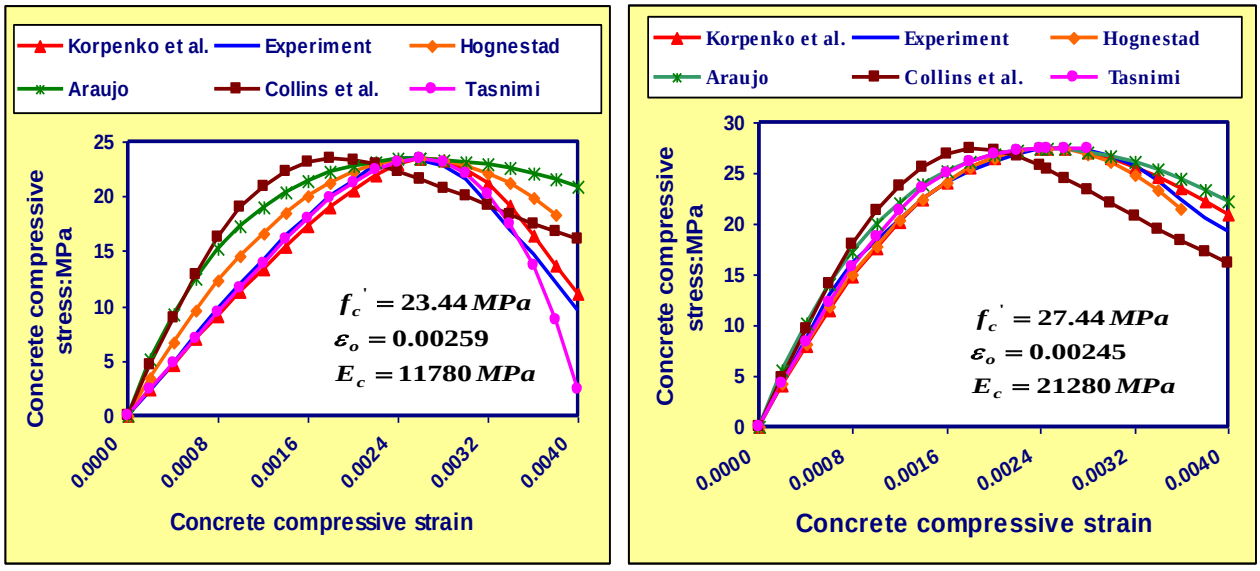

(a) (b)

Figure (4) Stress-strain for low strength concrete LSC:
(a) (Wang et al., 1978), (b) (Tasnimi, 2004)

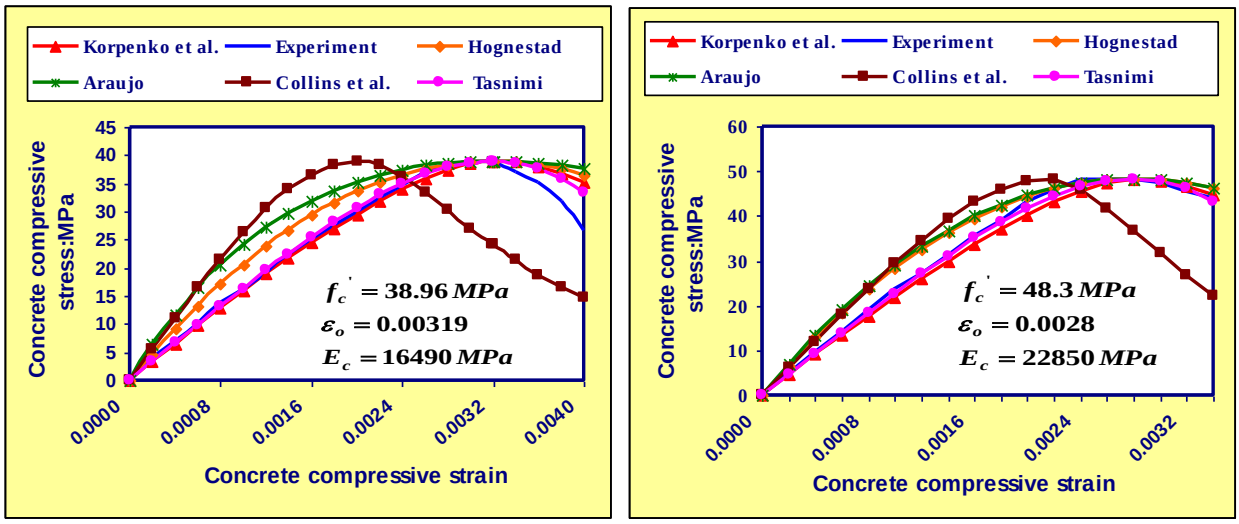

(a) (b)

Figure (5) Stress-strain for normal strength concrete NSC: (a) (Wang et al., 1978), (b) (Slate et al., 1986)

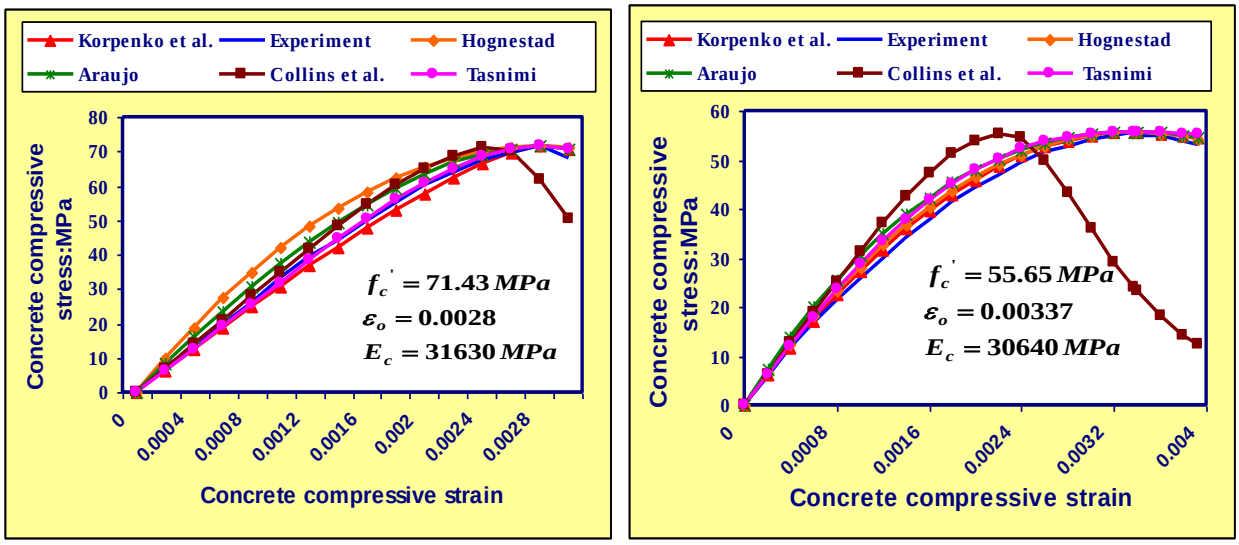

(a) (b)

Figure (6) Stress-strain for high strength concrete HSC: (a) (Slate et al., 1986), (b) (Tasnimi, 2004)

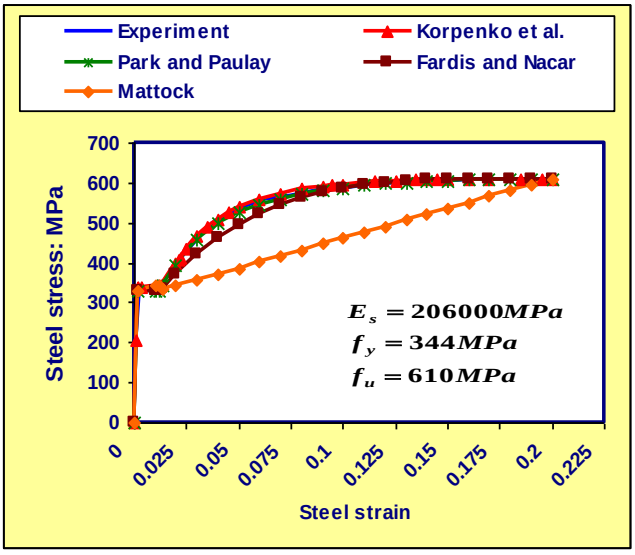

Figure (7) Stress-strain diagram for mild **steel** (Goto et al., 1998)

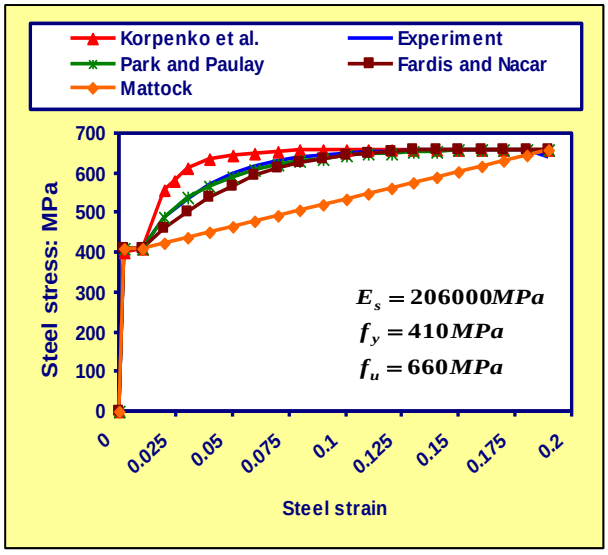

Figure (8) Stress-strain diagram for mild steel (Cho et al., 2004)

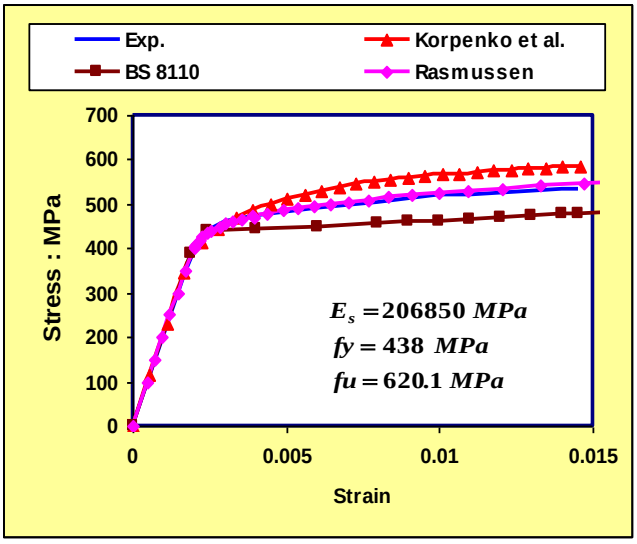

Figure (9) Stress-strain for mild steel (Tompos and Frosh, 2002)

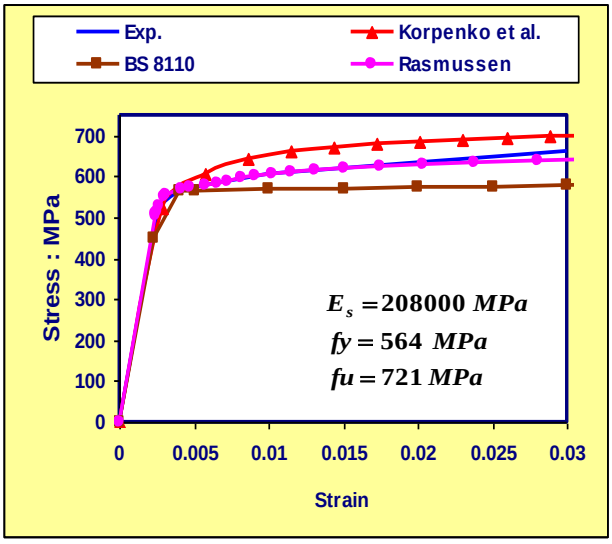

Figure (10) Stress-strain for mild steel (Kenel et al., 2005)

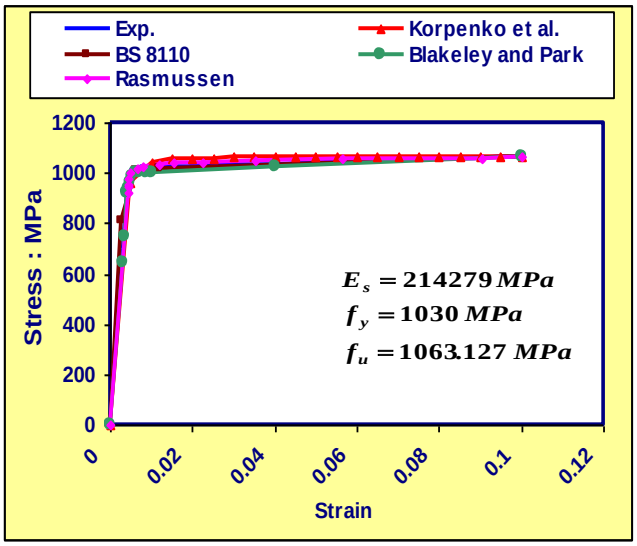

Figure (11) Stress-strain for HSS with prestressing (California Prestressing Manual, 2005)

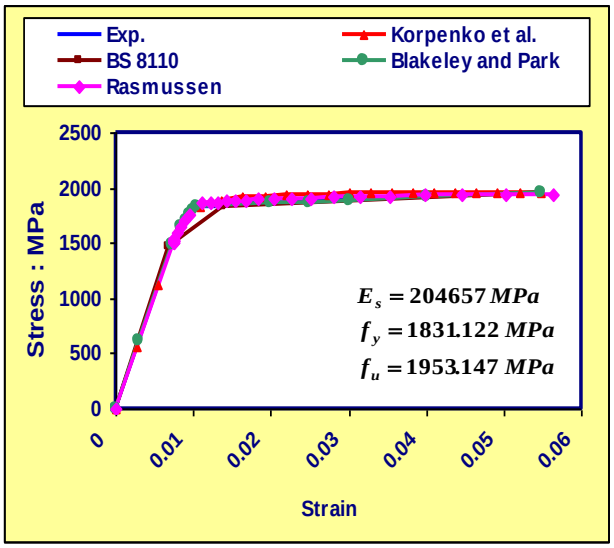

Figure (12) Stress-strain for HSS with prestressing (Canfield, 2005)

MODEL ASSUMPTIONS

The proposed model for calculating the deflection depends on the following assumptions:

- Strain in the concrete and reinforcement is proportional to the distance from the neutral axis (plane cross sections remaining plane after bending).
- Concrete behavior in compression and in tension and steel behavior are assumed to follow Korpenko's model Fig. (1) and Fig. (2).
- The tensile behavior of the FRP reinforcement is linearly elastic until failure stage. (Fig. 3).
- All stresses in concrete and steel are related to secant modulus of elasticity.
- Shear and torsion stresses are ignored.
- Perfect bond exists between concrete, steel reinforcement and FRP bars.

- Concrete is divided into a group of small cells with its number related to the required accuracy. Beside that, the longitudinal steel and FRP bars in the section are divided into a group of elements, with their numbers equal to the numbers of steel and FRP elements. Thus the structural element acts as a system of linear elements exposed to compression and axial tension.
- The beam is considered as simply supported with symmetrical shape along the vertical centerline of the beam. This includes the type of loading and the beam cross section.
- Newmark's numerical procedure is used to determine the deflection from the section curvatures along the beam.
- In the case of fully or partially prestressed concrete members, the positive value of deflection indicates downward displacement, and the negative sign indicates that the displacement is upward (i. e. camber).
- The component of the prestress along the beam axis is assumed constant, but the distance from the prestressing center of gravity to the global axis is taken according to the prestressing steel position in each section.

MOMENT-CURVATURE MODEL

A partially prestressed concrete member is taken as a case study for determining the moment-curvature relation of structural concrete members. The concrete is distinguished by the subscript (c), prestressed steel by (ps), non-prestressed steel by (s), and (f) for FRP.

The space that is occupied by the section is assigned by the symbol Ω. In this space, there are areas occupied by concrete, prestressed steel, nonprestressed steel, and FRP which are symbolized as A_c, A_{ps}, A_s, and A_f respectively, as shown in (Fig. 13).

$$\Omega = A_c + A_{ps} + A_s + A_f \tag{8}$$

The external force, which is either normal force (prestressing force) or applied load, leads to change the general form of the element causing strain distribution at individual sections.

The strain energy per unit length is determined by the following formula:

$$U^{(\ell)} = \frac{1}{2}\int_{\Omega} (\sigma\varepsilon + \tau\gamma)\, d\Omega \tag{9}$$

where

σ ، ε =normal strain and stress, respectively; γ ، τ =shear strain and stress, respectively.

The equation that relates the stress to strain is as follows:

$$\sigma = \bar{E}\,\varepsilon \tag{10}$$

where $\bar{E}$ = secant modulus of elasticity of the material, which takes into account the initial stresses and strains, and its calculation is based on $\sigma - \varepsilon$ diagrams for the materials as shown in Figs. (14) and (15).

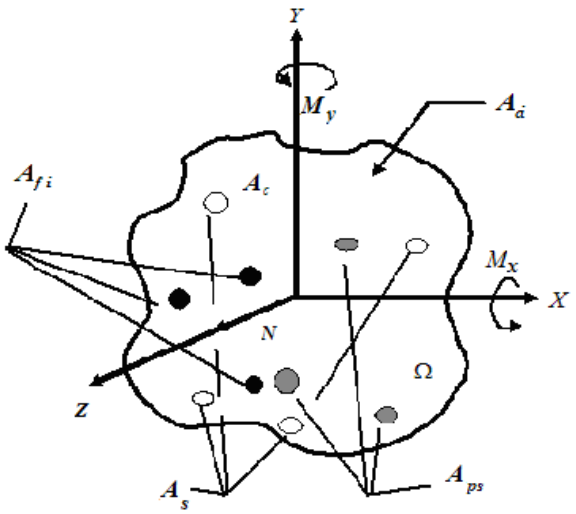

Figure (13) Cross-section of the structural element

$$\overline{E}=\begin{cases}\overline{E}_c\ , & x,y\in A_c\\ \overline{E}_{ps}\ , & x,y\in A_{ps}\\ \overline{E}_s\ , & x,y\in A_s\\ \overline{E}_f=E_f\ , & x,y\in A_f\end{cases} \tag{11}$$

Eq. (10) is substituted in Eq. (9). Shear stress and strain which appear in Eq. (9) are neglected (assumption No. 5).

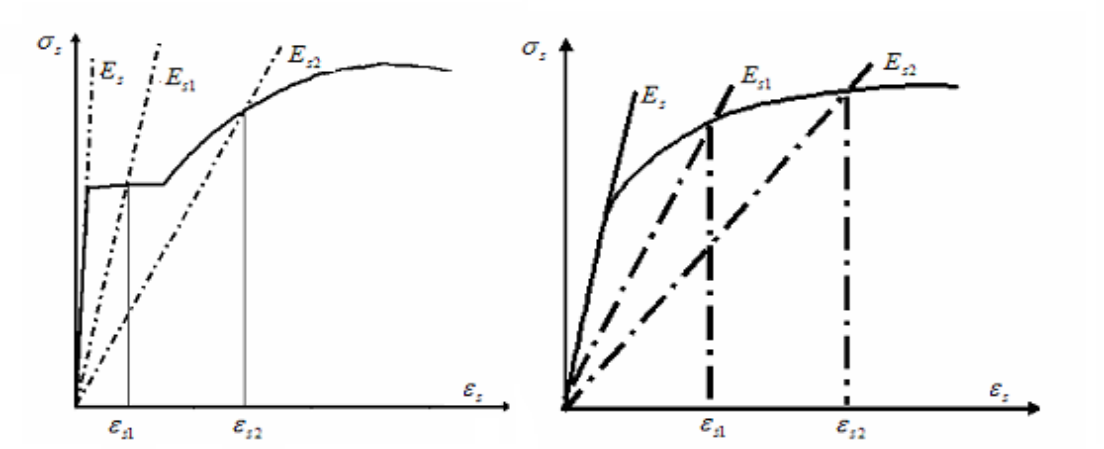

(a) (b)

Figure (14) Variation of secant modulus of elasticity, (a) for mild steel, (b) for high strength steel

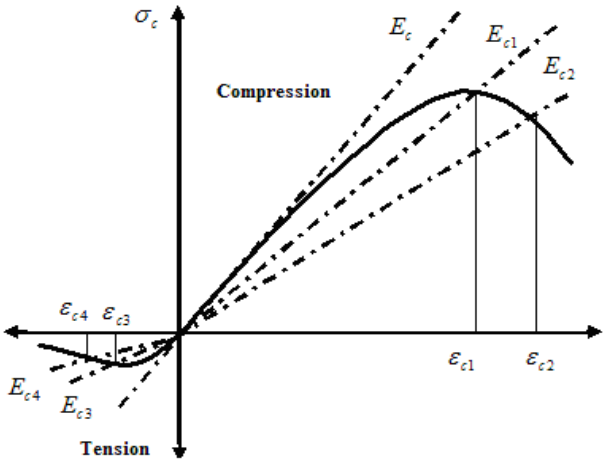

Figure (15) Variation of secant modulus of elasticity for concrete

So Eq. (9) takes the following form:

$$U^{(\ell)}=\frac{1}{2}\int_{\Omega}\varepsilon\bar{E}\varepsilon\,d\Omega \tag{12}$$

Because a linear strain distribution across the cross-section is assumed, so the third order vector will simulate the strain increment as in Eq. (13):

$$\varepsilon=\lambda^T Z \tag{13}$$

in which $\lambda=(\varepsilon_o,K_x,K_y)^T$, $Z=(1,y,x)^T$, λ = axial strain vector, ε_o = axial strain, K_x = curvature of the member longitudinal axis in OYZ plane, K_y = curvature of the member longitudinal axis in OXZ plane, x, y = the distance from the center of gravity of concrete, prestressed, non-prestressed steel, and FRP in the cross-section, to the selected reference coordinates.

By the assumption that a plane cross section before bending remains plane after bending, the strain at any point can be expressed by the following relationship:

$$\varepsilon=\varepsilon_o+K_x y+K_y x \tag{14}$$

Considering Eq. (13), then Eq. (12) becomes as:

$$U^{(\ell)}=\frac{1}{2}\int_{\Omega}\lambda^T Z\bar{E}Z^T\lambda\,d\Omega \tag{15}$$

A matrix C is defined as:

$$C=\int_{\Omega}Z\bar{E}Z^T d\Omega \tag{16}$$

C= stiffness matrix relative to the selected reference coordinates.

To identify the loads related to the resultant axial strains, partial differentiation of the strain energy equation is taken as:

$$\frac{\partial U^{(\ell)}}{\partial \varepsilon_o}=N=C_1\lambda\ ,\frac{\partial U^{(\ell)}}{\partial K_x}=M_x=C_2\lambda,\ \frac{\partial U^{(\ell)}}{\partial K_y}=M_y=C_3\lambda \tag{17}$$

where

N = Longitudinal force; M_x =bending moment in OYZ plane; M_y = bending moment in OXZ plane; C_1 = general axial stiffness vector; C_2 = general flexural stiffness vector in OYZ plane; C_3 = general flexural stiffness vector in OXZ plane.

The general axial stiffness vector C_1 is determined by the following equation:

$$C_1=\left(\int_\Omega \overline{E}\,d\Omega\ ,\int_\Omega \overline{E}\,y d\Omega\ ,\int_\Omega \overline{E}\,x d\Omega\right) \tag{18}$$

The flexural stiffness vectors C_2 and C_3 are limited by Eq. (19) and Eq. (20).

$$C_2=\left(\int_\Omega \overline{E}\,y d\Omega\ ,\int_\Omega \overline{E}\,y^2 d\Omega\ ,\int_\Omega \overline{E}\,x y d\Omega\right) \tag{19}$$

$$C_3=\left(\int_\Omega \overline{E}\,x d\Omega\ ,\int_\Omega \overline{E}\,x y d\Omega\ ,\int_\Omega \overline{E}\,x^2 d\Omega\right) \tag{20}$$

The direct integration of stiffness vectors elements C_1, C_2, and C_3 is unknown (not explicit) theoretically because the secant modulus of elasticity depends on the value of the resulted strains, and the strain gradient which is not equal to zero. Accordingly, numerical methods should be used. Therefore, the cross section is covered by a mesh mostly with perpendicular lines. Average value of the stress (strain) is taken in each cell. So the infinite summation of the elements of section stiffness matrix is substituted by a finite summation, that its maximum value is equal to the number of developed mesh cells.

Based on this, the matrix elements take the following form:

$$C_{11}=\sum_{i=1}^{k}\overline{E}_{ci}\,A_{ci}+\sum_{i=1}^{m}\overline{E}_{si}\,A_{si}+\sum_{i=1}^{n}\overline{E}_{psi}\,A_{psi}+\sum_{i=1}^{j}\overline{E}_{fi}\,A_{fi} \tag{21}$$

$$C_{12}=C_{21}=\sum_{i=1}^{k}\overline{E}_{ci}\,A_{ci}\,y_{ci}+\sum_{i=1}^{m}\overline{E}_{si}\,A_{si}\,y_{si}+\sum_{i=1}^{j}\overline{E}_{psi}\,A_{psi}\,y_{psi}\ +\sum_{i=1}^{n}\overline{E}_{fi}\,A_{fi}\,y_{fi} \tag{22}$$

$$C_{13}=C_{31}=\sum_{i=1}^{k}\overline{E}_{ci}\,A_{ci}\,x_{ci}+\sum_{i=1}^{m}\overline{E}_{si}\,A_{si}\,x_{si}+\sum_{i=1}^{n}\overline{E}_{psi}\,A_{psi}\,x_{psi}\ +\sum_{i=1}^{j}\overline{E}_{fi}\,A_{fi}\,x_{fi} \tag{23}$$

$$C_{22}=\sum_{i=1}^{k}\overline{E}_{ci}A_{ci}y^{2}_{ci}+\sum_{i=1}^{m}\overline{E}_{si}A_{si}y^{2}_{si}+\sum_{i=1}^{n}\overline{E}_{psi}A_{psi}y^{2}_{psi}+\sum_{i=1}^{j}\overline{E}_{fi}A_{fi}y_{fi}^{2} \quad (24)$$

$$C_{23}=C_{32}=\sum_{i=1}^{k}\overline{E}_{ci}A_{ci}x_{ci}y_{ci}+\sum_{i=1}^{m}\overline{E}_{si}A_{si}x_{si}y_{si}+\sum_{i=1}^{n}\overline{E}_{psi}A_{psi}x_{psi}y_{psi}+\sum_{i=1}^{j}\overline{E}_{fi}A_{fi}x_{fi}y_{fi} \quad (25)$$

$$C_{33}=\sum_{i=1}^{k}\overline{E}_{ci}A_{ci}x^{2}_{ci}+\sum_{i=1}^{m}\overline{E}_{si}A_{si}x^{2}_{si}+\sum_{i=1}^{n}\overline{E}_{psi}A_{psi}x^{2}_{psi}+\sum_{i=1}^{j}\overline{E}_{fi}A_{fi}x^{2}_{fi} \quad (26)$$

where:

C_{11}= axial stiffness, which depends on the loading level and the geometrical properties of the cross section, C_{12} =axial-flexural stiffness, which reflects the reciprocal influence of the longitudinal force with the bending moment in the direction of Y-axis, and it depends on the geometrical properties of the cross section, on the resultant stress-strain developments and on the location and direction of selected coordinates axes, C_{13}=axial-flexural stiffness, which reflects the reciprocal influence of the longitudinal force with bending moment in the direction of X axis, C_{22}=flexural stiffness in the direction of Y axis, C_{23}=the stiffness, which reflects the reciprocal influence of bending in the direction of the axes X and Y, and depends on the geometrical properties of the section, on the strain level and on the location of selected coordinates, C_{33}=flexural stiffness in the direction of X-axis, k =number of effective cells (strips) in concrete, A_{ci}=cross-sectional area of the concrete strip i, x_{ci},y_{ci}=the distance from the center of gravity of the concrete strip i to the selected coordinates, m=the number of non-prestressed longitudinal steel bars in the cross section, A_{si}= the cross-sectional area of non-prestressed longitudinal steel bar i, x_{si},y_{si} =the distance from the center of gravity of non-prtestressed longitudinal steel bar i to the selected coordinates; n =number of prestressed longitudinal steel bars in the cross-section; A_{psi} =the cross-sectional area of prestressed steel bar i ; x_{psi},y_{psi} =the distance from the center of gravity of prestressed longitudinal steel bar i to the selected coordinates, A_{fi}= the cross-sectional area of the FRP bar, x_{fi}, y_{fi} = the distance from the center of gravity of longitudinal FRP bar i to the selected coordinates, **j**=number of longitudinal FRP bars in the concrete cross-section.

The secant modulus of elasticity $\overline{E}$ can be expressed as:

$$\overline{E}=E\nu \quad (27)$$

where

E =the initial modulus of elasticity for the material (concrete, steel, or fiber);

ν = elastic strain factor and it expresses the ratios between the elastic strains to total strains (as given before).

The system (17) can be rewritten in another form to become:

$$\{F\}=[C(\lambda)]*\{\lambda\} \tag{28}$$

where $\{F\}$ = loads vector; $[C(\lambda)]$ =stiffness matrix of the section; $\{\lambda\}$ = strains vector.

The nonlinear system (28) is considered for determining the curvature of any cross-section in the concrete structural members. The elements of Eq. (28) change with changing the location of coordinates axis, it means that the axes rotate by an angle with certain value or at the time of moving the axes parallel to the existing axes (Fig. 13).

5. Evaluation of Strain Vector at Different Loading Cycles:

The solution of the nonlinear system (Eq. (28)) with the third order, which is specified to determine the curvature of any cross-section in the structural concrete members, depends on the iterative methods of numerical analysis. There are several numerical methods for converting the nonlinear Eq. (28) to linear. One of these methods is called the direct iterative technique (Cook, 1981), with its iteration diagram for solving Eq. (28), takes the following form as shown in Fig. (16).

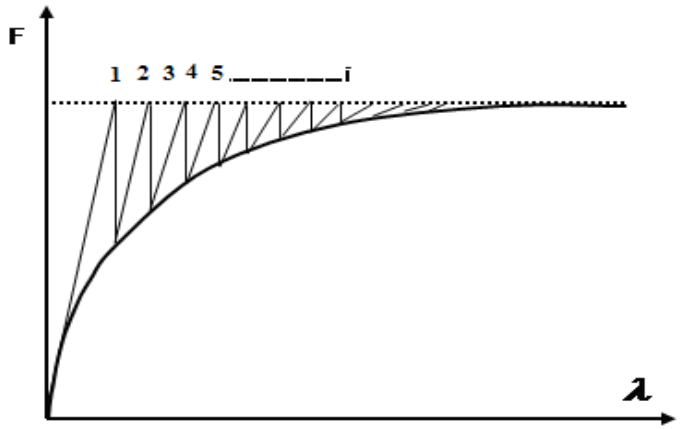

Figure (16) Iterative technique for solving the nonlinear equation (Cook, 1981)

In this method, full load is applied once at the first iteration and then a new stiffness matrix has to be formed in each iteration. Then the full system of Eq. (28) is solved in each iteration to evaluate the strain vector $\{\lambda\}$. Initially, a value of $\{\lambda\}=\{\lambda_o\}$ is assumed, then an improved approximation is obtained as:

$$\left.\begin{aligned} &\lambda_i = C^{-1}\,(\lambda_{i-1})*F \\ &\lambda_o = 0 \\ &i = 1,2,3,\ldots,\ldots,\ldots \end{aligned}\right\} \tag{29}$$

where λ_{i-1}, λ_i = axial strains vector in previous and current iteration cycles at one loading level, respectively.

To solve Eq. (29), a correction to the stiffness matrix should be done at each iteration cycle with fixing the vector of external applied loads.

NEWMARK NUMERICAL INTEGRATION

In the case of a symmetrical simply supported beam, the following Eqs. (30) can be used by considering the following symbols: ϕ referring to the curvature M/EI, $\bar{\phi}$ referring to the equivalent concentrated load (or curvature in the real beam), $slope_{(i)}$ referring to the shear (or average slope in the real beam between the points i and $i+1$, Δ referring to deflection, subscript i referring to section number, c referring to section number in the center of the beam, and Δx refers to segment length which is equal to the distance between two concentrated loads.

For a simply supported beam, there are no known values of $\bar{\phi}$ and slope in both ends; therefore these values can be substituted by zero.

$$\Delta_{(i)} = \sum_{j=2}^{i} (slope_{(j)})\,\Delta x \qquad (30)$$

where i =1,2,3,…, $c-1$

$slope_{(j)} = \sum_{k=2}^{c-1} \bar{\phi}_{(k)} + \bar{\phi}_{(c)} / 2$, where $slope_{(j)}$ is dimensionless

$\bar{\phi}_{(k)} = \frac{\Delta x}{6}\left(\phi_{(k-1)} + 4\phi_{(k)} + \phi_{(k+1)}\right)$ for straight line curvature (M/EI).

$\bar{\phi}_{(k)} = \frac{\Delta x}{12}\left(\phi_{(k-1)} + 10\phi_{(k)} + \phi_{(k+1)}\right)$ for 2nd degree parabolic curvature (M/EI).

Since the beam is symmetric the values of deflection for other half of the beam is determined according to the following formula:

$\Delta_{p+1} = \Delta_{n-p}$

where p =1,…c-1, n = number of sections along the beam.

APPLICATIONS AND RESULTS

Ordinary reinforced concrete beams

Beam SB1-2 is tested by Thandamoorthy (1999). This beam had 150*300 *mm* section, 3m span length, the ultimate compressive strength for concrete ($f_c' = 41.58\,MPa$). The beam is reinforced with $3\Phi 12$ bars in tension with an effective depth of 261 *mm* and $2\Phi 8$ bars in compression with depth of 37 *mm* and with E_s equal to 200000 *MPa* .The beam has been loaded in two points. Loading points have been located at 500 *mm* on either side of midspan. Moment-curvature and load-deflection diagrams of this beam are shown in Figs. (17 and 18).

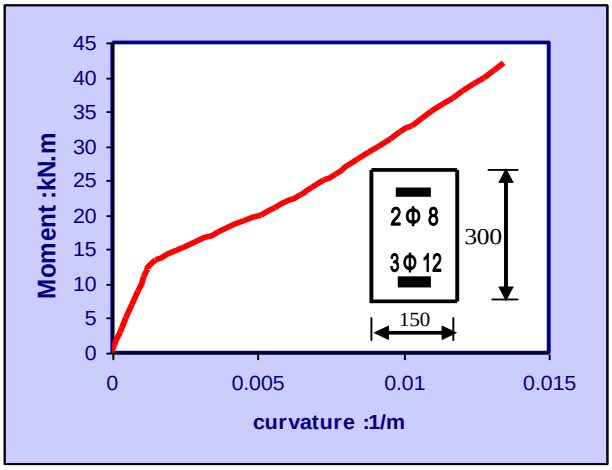

Figure (17) Theoretical moment-curvature diagram for Thandamoorthy beam

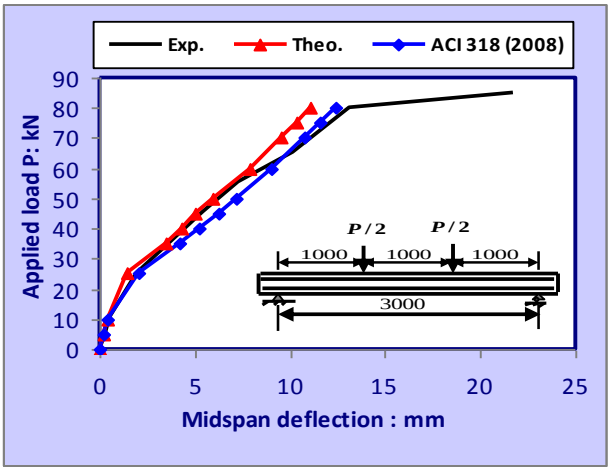

Figure (18) Load-deflection diagram (Thandamoorthy, 1999)

GB1 control beam is tested by Alsayed, et al., (2002). The typical beam is 150*200 *mm* in cross-section. It is reinforced with three $\Phi 10\,mm$ steel bars for tension with an effective depth of 152 *mm* and one $\Phi 6\,mm$ for compression with depth of 46 *mm* and with E_s equal to 200000 ***MPa***. The beam is simply supported over a span of 2050 *mm* and loaded by two concentrated loads, each placed at 100 *mm* from the beam centerline. The ultimate compressive strength for concrete is ($f_c^{'} = 35.5\,MPa$). Moment-curvature and load-deflection diagrams of this beam are shown in Figs. (19 and 20).

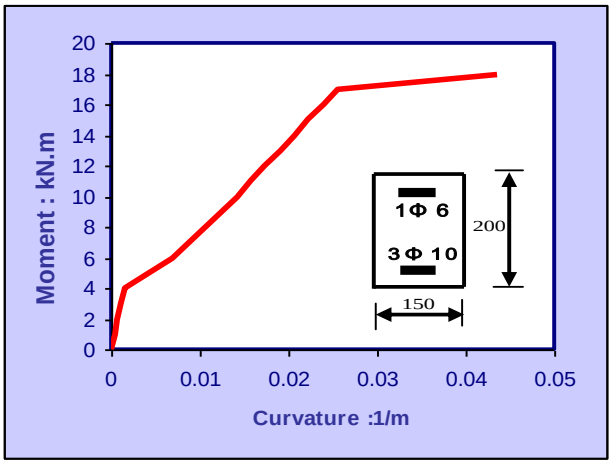

Figure (19) Theoretical moment-curvature diagram for Alsayed et al. beam

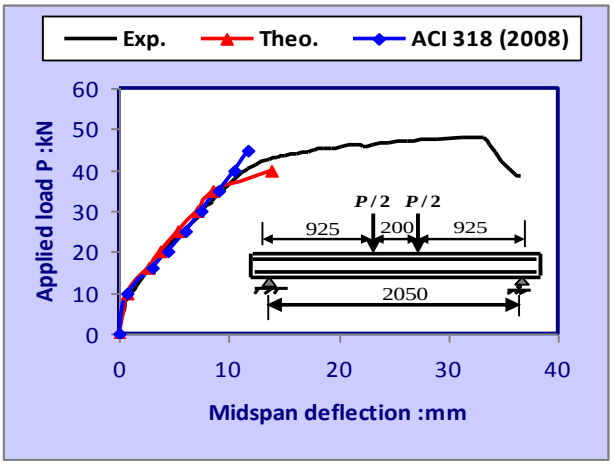

Figure (20) Load-deflection diagram (Alsayed et al., 2002)

<u>Partially prestressed concrete beam</u>

Beam SSP2 was tested by Harajli and Naaman (1985). The beam has 2743.2 *mm* span length. The ultimate compressive strength for concrete is ($f_c^{'} = 36.55\,MPa$).It was subjected to two-point loading. The cross-section was 114.3*228.6 *mm* in dimensions. It was with ordinary tensile reinforcement of area 96.774 mm^2 with an effective depth of 203.2 *mm* and a tensile prestressing strand of area 54.839 mm^2 with an effective depth of 158.75 *mm*. Moment-curvature and load-deflection diagrams of this beam are shown in Figs. (21 and 22).

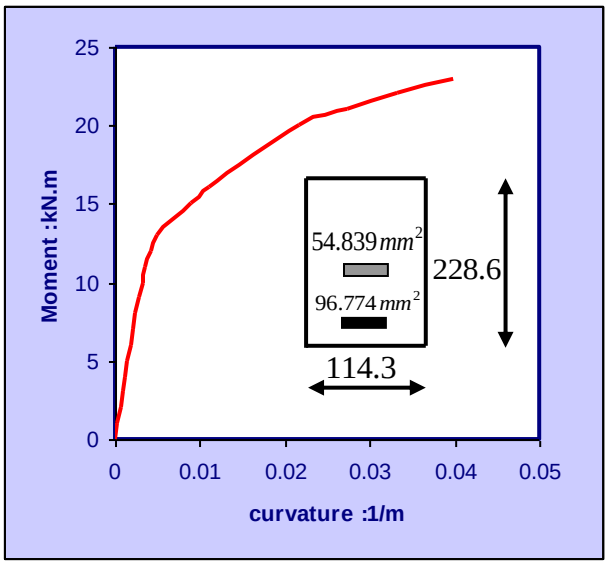

Figure (21) Theoretical moment-curvature diagram for Harajli and Naaman beam

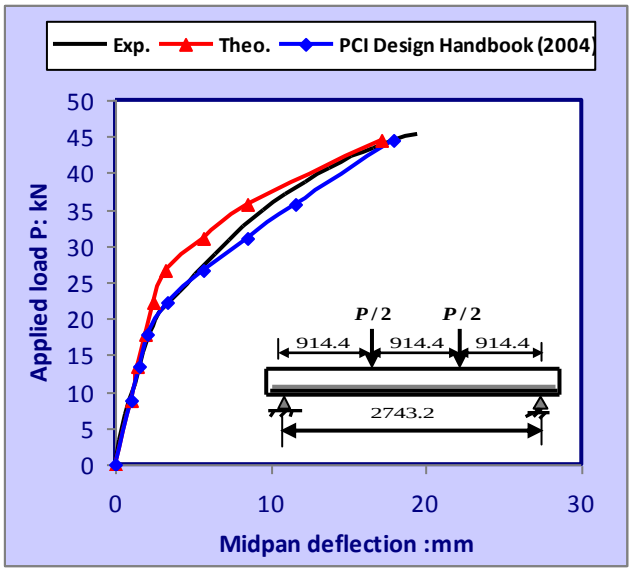

Figure (22) Load-deflection diagram (Harajli and Naaman, 1985)

The beam (beam III-2) was tested by Oukaili (1991). The cross-section was 210*305 *mm*. The beam was reinforced in tension with steel of area 907 mm^2 with an effective depth of 275 *mm* and prestressing strand of area 420.27 mm^2 at a depth of 235 *mm*. It is also reinforced in compression with steel area of 157 mm^2 and prestressing strand area of 96. 535 mm^2 at a depth of 30 *mm*. The ultimate compressive strength for concrete is ($f_c^{'} = 39.4\,MPa$).Moment-curvature and load-deflection diagrams of this beam are shown in Figs (23 and 24).

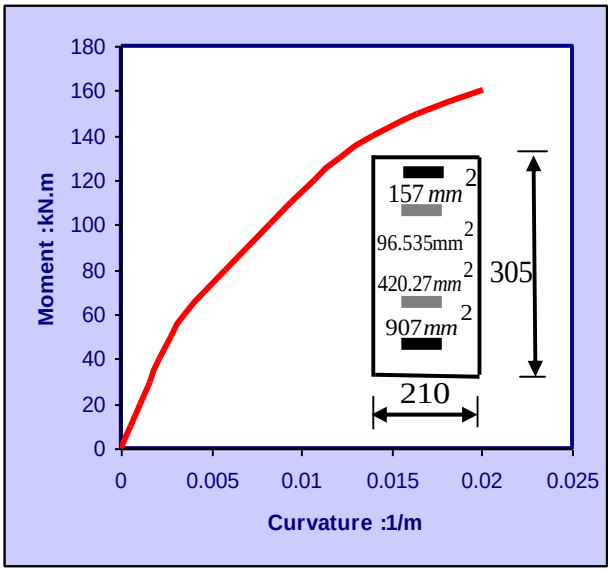

Figure (23) Theoretical moment-curvature diagram for Oukaily beam

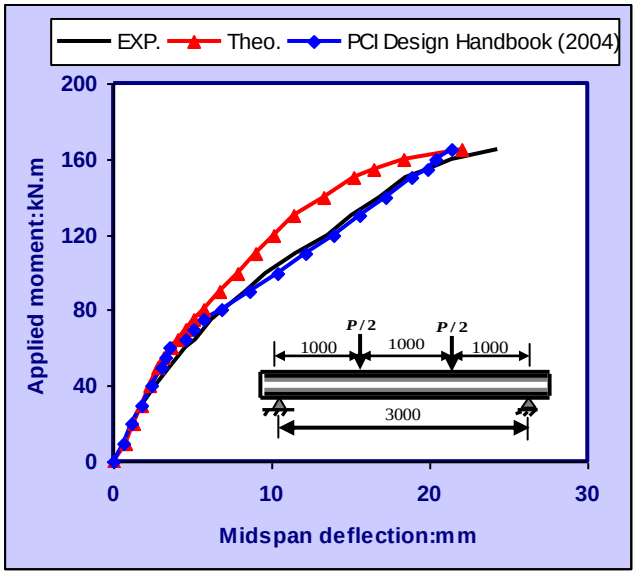

Figure (24) Load-deflection diagram (Oukaily, 1991)

Beams Reinforced with GFRP

Benmokrane et al. (1996) built a series of 3300 *mm* long doubly reinforced concrete beams. Series 1 is taken for comparison. The beam tested had two Φ 19.1 *mm* GFRP bars in tension and two Φ 6 *mm* GFRP bars in compression. The beam section was 200*300 mm. It had a clear span of 3000 mm and was loaded by two concentrated loads each at 500 mm from midspan. The ultimate

compressive strength for concrete was ($f_c^{'} = 43\,MPa$). Moment-curvature and load deflection diagrams of this beam are shown in Figs (25 and 26).

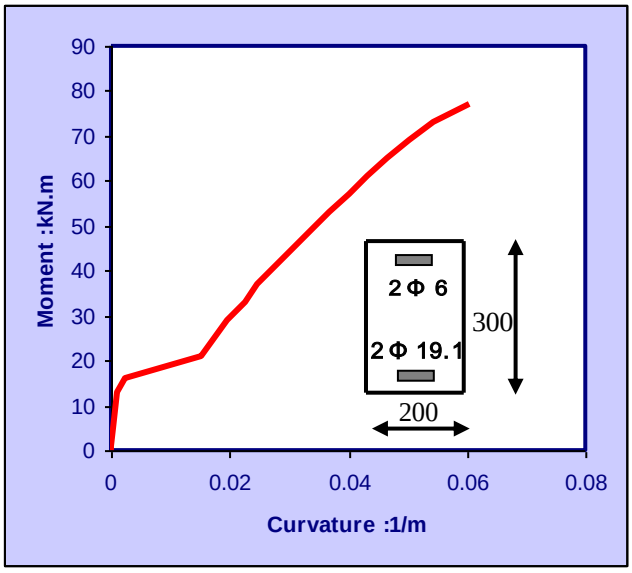

Figure (25) Theoretical moment-curvature diagram for Benmokrane et al. beam

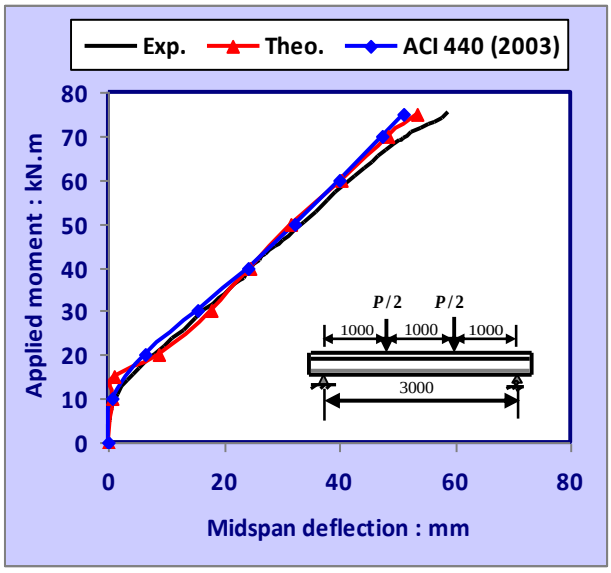

Figure (26) Load-deflection diagram (Benmokrane et al., 1996)

Beam F3 tested by Pecce et al., (1998) has 500*185 mm in cross section, reinforced with seven Φ 12.7 mm GFRP bars in tension at a depth of 145 *mm* and two Φ 12.7 mm GFRP bars in compression at a depth of 40 mm. The clear span of the beam is 3400 *mm*, and it is loaded by two concentrated loads at 1200 *mm* from the simple supports. The ultimate compressive strength for concrete is ($f_c^{'} = 30\,MPa$).The theoretical moment-curvature and load-deflection diagrams are shown in Figs. (27 and 28).

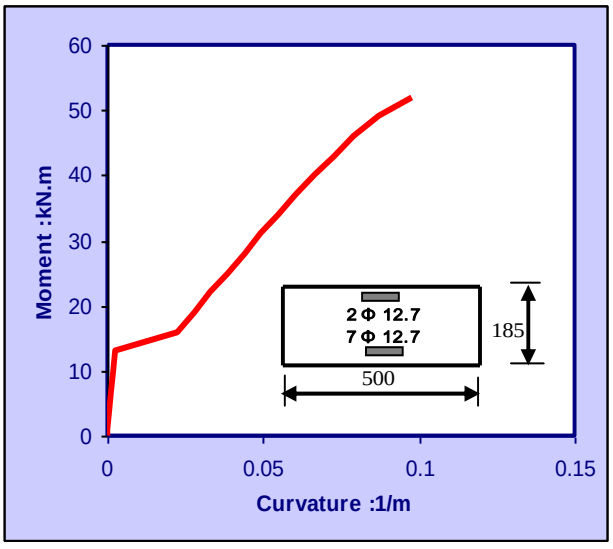

Figure (27) Theoretical moment-curvature diagram for Pecce et al. beam

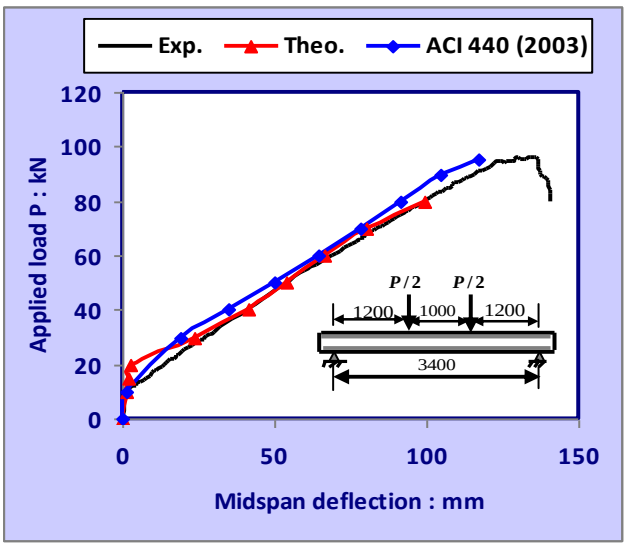

Figure (28) Load-deflection diagram (Pecce et al., 1998)

CONCLUSIONS

The following conclusions can be stated:

- The analytical stress-strain model used in the SECTION program which was developed by Korpenko et al., (1986) gave very good agreement in comparison with the experimental data and other analytical models for each of concrete, mild steel, high strength steel, and prestressing steel.
- SECTION program presented in this study has shown to be capable of predicting the full history for the structural concrete beams under short-term loading.
- The SECTION program has the ability of dealing with structural beams with different values of partial prestressing ratio (PPR).
- The SECTION program has shown to be capable of predicting the deflection state for each of ordinary reinforced concrete, partially prestressed concrete, and bar fiber reinforced concrete beams.
- In the pre-crack stages, there is very good agreement between the theoretical results and the experimental data of deflection for all the three types of beams used.
- In the loading stages corresponding to 20% of the failure load, the average discrepancy of the analytical deflections values with respect to experimental values reached 18.3% for ordinary reinforced concrete, 4.9% for partially prestressed concrete beams, and 24.92 % for beams reinforced with fiber bars. One problem that seems to be common to all deflection prediction methods is that of predicting the cracking moment. This is primarily due to the difficulty in accurately predicting the modulus of rupture f_r (standards tend to require the use of relatively low conservative values).
- In the loading stages corresponding to 50% from the failure load, the average discrepancy of the analytical deflections values with respect to experimental values reached 6.83% for ordinary reinforced concrete, 27.4% for partially prestressed concrete beams, and 8.73% for beams reinforced with fiber bars.
- In the loading stages corresponding to 70% of the failure load, the average discrepancy of the analytical deflections values with respect to experimental values reached 8.63% for ordinary reinforced concrete, 30.75% for partially prestressed concrete beams, and 7.45% for beams reinforced with fiber bars.

NOTATIONS:

The following symbols are used in this paper:

$\boldsymbol{e_{1c}}, \boldsymbol{e_{2c}}$ =Factors expressing the type of the concrete.

$\boldsymbol{e_{1s}}, \boldsymbol{e_{2s}}$ = Factors expressing the type of the steel.

$\overline{\boldsymbol{E}}$ = secant modulus of elasticity of the material.

$\boldsymbol{E_c}$ = Modulus of elasticity of concrete.

$\boldsymbol{E_s}$ = Modulus of elasticity of reinforcing steel.

$\boldsymbol{f_c'}$ =Ultimate compressive strength of concrete.

HSC =High Strength Concrete.

HSS = High Strength Steel.

$\boldsymbol{K}$ = Curvature.

$\boldsymbol{K_x}$ =Curvature about x-axis.

$\boldsymbol{K_y}$ = Curvature about y-axis.

LSC =Low Strength Concrete.

$\boldsymbol{M_x}$ =Bending moment in OXZ level.

M_y =Bending moment in OYZ level.

N =Normal force.

NSC =Normal Strength Concrete.

U =Strain energy.

Δ =Deflection.

ε =Strain.

ε_c =Strain corresponding to σ_c .

$\tilde{\varepsilon}_c$ =Concrete strain level.

$\hat{\varepsilon}_c$ =The concrete strain corresponding to $\hat{\sigma}_c$.

$\varepsilon_{c,el}$ =Strain corresponding to $\sigma_{c,el}$.

$\tilde{\varepsilon}_{c,el}$ =Strain corresponding to $\tilde{\sigma}_{c,el}$.

ε_{fu} =FRP ultimate strain.

ε_s =Strain in steel.

ν_c =Concrete elastic modulus factor that expresses the ratio of elastic strains to the total strains.

ν_o =Factor depending on stress level in the material.

ν_s = Steel elastic modulus factor that express the ratio of elastic strains to the total strains.

σ =Stress.

σ_c =Concrete compressive stress.

$\hat{\sigma}_c$ =Concrete ultimate compressive strength.

$\tilde{\sigma}_c$ =Concrete stress level.

$\sigma_{c,el}$ =Elastic concrete stress.

$\tilde{\sigma}_{c,el}$ = The level of elastic concrete stress.

σ_{fu} =FRP ultimate stress.

σ_s =Stress in steel.

$\tilde{\sigma}_s$ = Steel stress level.

$\sigma_{s,el}$ = Elastic steel stress.

$\tilde{\sigma}_{s,el}$ = The level of elastic steel stress.

Ω = Space occupied by the section.

REFERENCES:

- ***ACI Committee 116***, "Cement and Concrete Terminology", American Concrete Institute, March 1, 2000.
- ***ACI Committee 318***, "Building Code Requirements for Structural Concrete (ACI 318-08) and Commentary (ACI 318R-08)", American Concrete Institute, Farmington Hills, 465 pp, 2008.
- ***ACI Committee 440***, "Guide for the Design and Construction of Concrete Reinforced with FRP Bars", Detroit: American Concrete Institute, 2003.

- ***Alsayed, S. H.***, ***Al Salloum, Y. A.*** and ***Almusallam, T. H***, "Rehabilitation of the Infrastructure Using Composites Fabrics", Final report, KACST, Riadh, Saudi Arabi, 2002 as cited in (Alsayed, S. H., Al Salloum, Y. A. and Almusallam, T. H.," FRP Composites as an Alternative Material to Strengthen, Upgrade and Repair of Infrastructure", The 6th Saudi Engineering Conference, KFUPM, Dhahran, December, Vol. 3, 2002.
- ***Araujo, J. M.***, modelo para analise de vigas de concreto armado. Revista, Portuguesa de Engenharia de Estruturas, Lisboa, Portugal, N. 32, P. 9-14, 1991, as cited in (Jose Milton de Araujo, "Simplified Procedures for Calculation of Instantaneous and Long-Term Deflections of Reinforced concrete Beams," Numero 24, 2005).
- ***Benmokrane, B***., ***Challal, O***. and ***Masmoudi, R.***," Flexural Response of Concrete Beams Reinforced with FRP Reinforcing Bars", ACI Structural Journal 91(2),1996, pp. 46-55 as cited in (Rim Nayal and Hayder A. Rasheed," Tension Stiffening Model for Concrete Beams Reinforced with Steel and FRP Bars", Journal of Materials in Civil Engineering , Vol. 18, No. 6, pp.831-841, December, 2006.
- ***Blakeley, R. W. G.*** and ***Park, R.***," Prestressed Concrete Sections with Seismic Loading", Journal of the Structural Division, ASCE, Vol.99, ST8, pp. 1717-1742, August, 1973.
- ***BSI (1997)***, "Structural Use of Concrete–Part 1: Code of Practice for Design and Construction (BS8110-1:1997), including amendments No. 1 (1998) and 2 (2002)", British Standards Institution, 1997, 163 pp.
- **California Prestressing Manual**, "A Guide for Field Inspection of Cast- in- Place Post-Tensioned Structures", State of California Department of Transportartation Engineering Services, January, 2005.
- **Canfield**, **Scott R.** "Full Scale Testing of Prestressed, High Performance Concrete, Composite Bridge Girders", M. S. C. Thesis, Georgia Institute of Technology, August 2005.
- ***Cho***, ***Jae-Yeol***, ***Kim***, ***Nam-Sik, Cho***, ***Nam-So,*** and ***Choi***, ***K.***," Cracking Behavior of Reinforced Concrete Panel Subjected to Biaxial Tension", ACI Structural Journal, Vol. 101, No. 1, pp.76-84, January-February 2004.
- ***Collins, M. P., Mitchell, D.,*** and ***MacGregor, J. G.***, " Structural Design Considerations for High-Strength Concrete", Concrete International, Vol. 15, No. 5, pp.27-34, May, 1993, as cited in (Sungjin Bae and Oguzhan Bayrak, "Stress Block Parameters for High Strength Concrete Members", ACI Structural Journal, Vol. 100, No. 5, pp.626-636, September-October, 2003).
- ***Cook R.D.***, "Concept and Application of Finite Element Analysis", Second Edition, John Wiley and Sons, New York, 1981.
- ***Fardis***, ***Michel N.*** and ***Nacar,*** **A.**,"Static Ultimate Capacity of R/C Containment", Journal of Structural Engineering, Vol. 110, No.5, May, pp. 961-977, 1984.
- ***Goto, Y.***, ***Wang, Q.***, and ***Obata, M.,***" FEM Analysis for Hysteric Behavior of Thin-Walled Columns", ASCE, Vol. 124, No. 11, pp. 1290-1301, 1998.
- ***Harajli, M. H***., and ***Naaman, A. E.***, Static and Fatigue Tests on Partially Prestressed Beams", Journal of the Structural Division, ASCE, Vol.111, No.7, July 1985, as cited in (Ali S. Alameh and Mahmed H. Harajli, 1989).
- ***Hognestad, E.***, "A Study of Combined Bending and Axial Loads in Reinforced Concrete Members", University of Illinois Engineering Experimental Station, Bulletin Series No. 399, November, 1951, as cited in (Park and Paulay, 1975).
- ***Korpenko, N. I.***, ***Mukhamediev, T.A.*** and ***Petrov, A. N.***, "The Initial and Transformed Stress - Strain Diagrams of Steel and Concrete. " Special Publication, Stress-Strain

Condition for Reinforced Concrete Construction, Reinforced Concrete Research Center, Moscow, 7 – 25, 1986, as cited in (Oukaili, 1997).

- ***Mattock, A.H.***, "Rational Capacity of Hinging Regions in Reinforced Concrete Beams", Flexural Mechanics of Reinforced Concrete, Proceedings of the international symposium, Miami, Fla, Nov. 1964, pp. 10-12 as cited in (Mukhlis Yousif Kettoola," Flexural Behavior of Composite Reinforced Concrete Beams", M. Sc. Thesis, University of Basrah, December, 1982).
- ***Newmark, N. M.,***"Numerical Procedure for Computing Deflections, Moments, and Buckling Loads", Transactions, ASCE, 1-8, 1943.
- ***Oukaili, Nazar K. Ali***," Strength of Partially Prestressed Concrete Elements with Mixed Reinforcement by Highly Strength Strands and Steel Bars", PH.D. Thesis, Moscow Civil Engineering University, Moscow, 1991.
- ***Oukaili, Nazar K. Ali***, "Moment Capacity and Strength of Reinforced Concrete Members Using Stress-Strain Diagrams of Concrete and Steel", Journal of King Saud University, Vol. 10, pp. 23-44, 1997 (in Arabic).
- ***Park, R.*** and ***Paulay T.***," Reinforced Concrete Structures", a Wiley Interscience Publication, John Wiley &sons. New York 1975.
- ***PCI Design Handbook***, Sixth Edition, Chicago: Prestressed Concrete Institute, 2004.
- ***Pecce, M.***, ***Manfredi***, ***G.*** and ***Cosenza, E***.," Experimental Behavior of Concrete Beams Reinforced with Glass FRP bars", Proc. 8th Eur. Conf. on Compos. Mat. Woodhead Publishing Limited, Cambridge U. K., 227-234, 1998 as cited in (*M. Pecce*, *G. Manfredi* and *E. Cosenza*," Experimental Response and Code Models of GFRP RC Beams in Bending", Journal of Composites for Construction, Vol. 4, No. 4, pp.182-190, November, 2000.
- ***Rasmussen***, ***Kim JR.,*** "Full-Range Stress-Strain Curves for Stainless Steel Alloys", The University of Sydney, Department of Civil Engineering, Center for Advanced Structural Engineering, Research report no. R811, November 2001.
- ***Tasnimi***, ***A. A.,***" Mathematical Model for Complete Stress-Strain Curve Prediction of Normal, Light-Weight and High-Strength Concretes", Magazine of Concrete Research, 56, No.1, pp.23-34, February, 2004.
- ***Thandavamoorthy***, ***T.S.,*** "Static and Fatigue of High-Ductility Bars Reinforced Concrete Beams", Journal of Materials in Civil Engineering, Vol. 11, No.1, February 1999.
- ***Tompos, E. J.*** and ***Frosh,*** **R. J.** " Influence of Beam Size, Longitudinal Reinforcement, and Stirrup Effectiveness on Concrete Shear Strength", ACI Structural Journal, Vol. 99, No. 5, pp.559-567, September-October, 2002.